KTH
Kungliga Tekniska Högskolan

SH2702 - Nuclear Reactor Technology
Master programme in Nuclear Energy Engineering

AP 1000

Team 51
Nicolas Andrade
Ian Gilley

March 6, 2023

Abstract

This paper describes general details of the AP1000 reactor, operation principles, and safety features. It then calculates thermal hydraulic parameters for the fuel assemblies in average and hot channels assuming a cosign heat distribution. Finally, we found the location of hot spots in the central channel and calculated the max fuel and cladding temperatures.
Keywords: AP-1000, passive safety systems, critical heat flux.

Contents

List of Figures

1 Task 1 - General design specification of the nuclear power plant with selected reactor type

1.1 Task description

In this task a literature study should be performed to find the general description of the reactor core, reactor vessel, primary/secondary loop, balance of plant, etc. The focus should be on the particular features that make the design unique and interesting.

1.2 Design specifications

The AP1000 is a Gen-III+ pressurized water reactor developed by Westinghouse. Its predecessor, the AP600 design, was created in the late 1980s post Three Mile Island as a response to the expectations set by the US power utilities for the next generation of nuclear power plants (NPP). Newer designs were expected to lower their core damage frequency, which was frequently achieved by adding redundant safety features (up to 4 independent trains per safety function). However, this leads to diminishing returns, common cause failure, seismic issues and significant seismic building cost. On top of that there is an increased complexity and higher operation and maintenance costs [1]. Consequently, the AP1000 was conceived to achieve its goals through passive safety systems. This Gen-III+ NPP has passive safety systems which can achieve and maintain safe shutdown for 72 hours following a Design Basis Event without requiring operator action [2].

Table 1: Main parameters AP1000

Parameter	**AP1000**
Net electric output, MWe	1117
Reactor power, MWt	3415
Hot leg temperature, °C (°F)	321 (610)
Number of fuel assemblies	157
Type of fuel assembly	17×17
Active fuel length, m (ft)	4.3 (14)
Linear heat rating, kW/ft	5.71
Control rods/Gray rods	53/16
R/VID., cm (in)	399 (157)
Vessel flow (thermal), 10^3 m^3/hr (10^3 gpm)	68.1 (300)
Steam generator surface area, m^2 (ft^2)	11,600 (125,000)
Pressurizer volume, m^3 (ft^3)	59.5 (2100)

The AP1000 is an advanced pressurized water reactor with a conventional 2-loop, 2 steam generator primary system configuration, rated at 3400 MWt and 1117 MWe. Its main characteristic is the use of passive safety systems, as opposed to active systems (e.g., pumps), to achieve and maintain safe shutdown. Passive systems are those that rely on pressure differences, gravity, convection and all other naturally occurring physical phenomena. The core and the containment itself are cooled down in case of accident through the passive emergency core cooling system, and the containment cooling system, respectively. The main design parameters are listed on

Figure 1: Containment building of the AP1000.

Table 1, while the containment vessel and building can be seen on Figure 1.

In order to increase the reliability of the design and not depend entirely on simulations and probabilistic risk assessments, but rather build on years of proven experience, the AP1000 uses components from other designs and adds a few minor tweaks and improvements. For example, the reactor vessel internals are those of the Belgian Doel 4 and Tihange 3 NPPs. The fuel is from South Texas 1 & 2, the steam generators from San Onofre, Waterford and Palo verde, and the pressurizer is used in 70+ plants worldwide [3].

Finally, to reduce its costs and complexity, compared to a standard G-III design, the AP1000 has 35% fewer safety grade pumps, 80% less safety class piping, 55% fewer piping penetrations in the containment, 50% fewer ASME safety class valves and 85% less cabling [4]. Moreover, its modular design and construction allow it to be a much more compact plant than earlier designs. Utilizing less than <10,000 m^3 of concrete and <1,200 MT of rebar, resulting in a reduction of the seismic building volume by 45%. There is no need for AC power during accidents since all power would be provided by class 1E batteries in case of an accident [5]. Lastly, the relatively large pressurizer makes it more accommodating to transients and therefore more forgiving to operate.

Figure 2 depicts the main features of the AP1000 vessel internals. Where the blue text describes the main enhancements with respect to the original Robust Fuel Assembly 2 design (RFA 2), and the red text describes the further improvements applied specifically to the AP1000. The top mounted instrumentation allows for easier handling and removal during refueling, the 4 extra intermediate flow mixers improve the heat transfer, the bottom fuel rod plenum improves the structural integrity and the low profile DFBN filters any possible harmful particle intake to

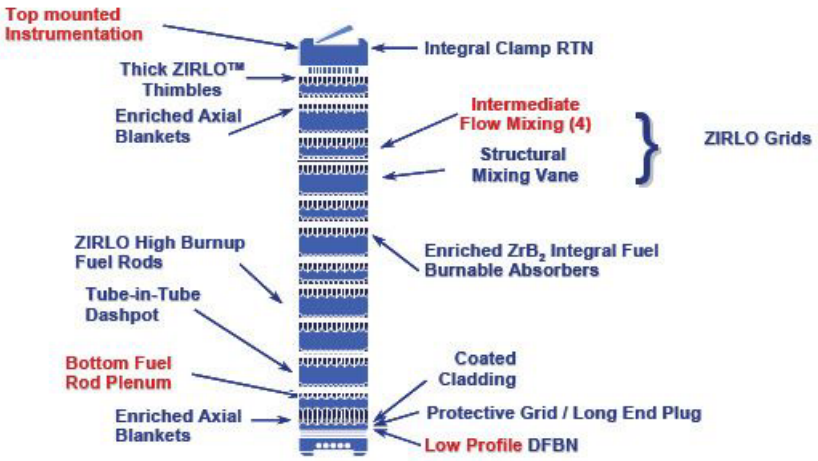

Figure 2: Reactor vessel internals AP1000.

the reactor. Regarding the UO_2 fuel, there are 3 radial regions of ^{235}U enrichment varying from 2.35% to 4.8%. The reactor operates on a 18-month fuel cycle with a 93% capacity factor.

Figure 3 allows us to visualize the primary system of the reactor, composed of a 2-loop, 2 steam generator design. The large pressurizer allows the system to maintain stable operation over a wider range of conditions as it can compensate more easily for transients. Additionally, the elongated surge line prevents the electric heaters from the pressurizer to influence the operation temperature of the reactor. The use of canned pumps allows for a leakage-free system. In addition, their intake is directly integrated into the steam generators as a way to reduce piping.

Finally, the secondary loop and balance of plant of the AP1000 does not differ with that of a standard PWR. There is a high pressure turbine and a low pressure turbine with intermediate reheating and moisture separation units.

2 Task 2 - Operational principles of the power plant

2.1 Task description

In this task we were directed to describe how the reactor was operated during start-up, normal operation, and shutdown. This includes base load and load-following scenarios, and the role and principles of operation of auxiliary systems, while focusing on unique and interesting features [6].

2.2 Operational principles

Starting in hot standby, with K_{eff} ¡ 0.99, and the average reactor coolant temperature ¿215.6 °C, the reactor is in normal operational state, but not critical. There is a steam bubble in the pressurizer, labeled at (10) in Fig. 4, which is maintained to provide pressure to the primary coolant. The chemical and volume control system (CVS) is used to maintain the concentration of boron high enough that the reactor

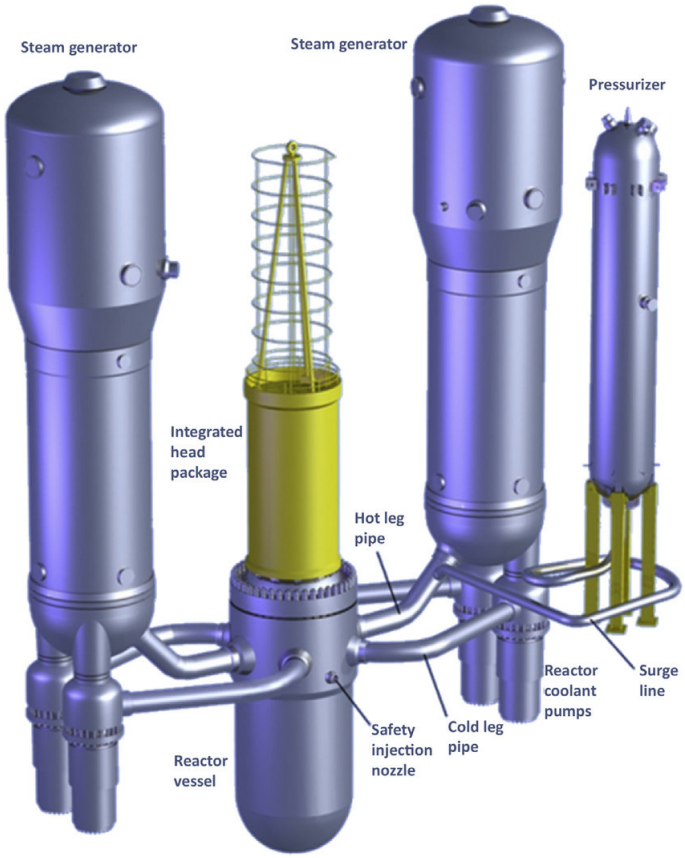

Figure 3: Primary loop AP1000.

does not become critical. Decay heat is removed by both steam generators (SG), showing in Fig. 4 flanked by the reactor coolant pumps (RCP). As the reactor is transitioned to start up, which is defined as reactivity ¿0.99 and ¡5% of rated thermal power. The CVS removes boron, and the black control rods are withdrawn to increase reactivity. Then the reactor can be transitioned to power operation, defined as K_{eff}¿ 0.99, and greater than 5% of rated thermal power. To maintain reactivity, the CVS controls boron concentration to account for fuel burn-up, while grey control rods move to change reactivity on short time scales. During power operations, the SGs provide steam at 56 bar and 271 °C to the turbines. To transition to safe shutdown, defined as K_{eff} ¡0.99, and average reactor coolant temperature between 215 °C and 93.3 °C, the CVS increases boron concentration, and decay heat is first removed by the SGs until the RC is below 176 °C and 31 bar, when the normal residual heat removal system (RNS) is used to remove decay heat. During cold shutdown, defined as K_{eff} ¡ 0.99, and average RC temperature below 93.3 °C, the RNS continues to control heat removal, and the CVS continues to control criticality. The gray control rods are an important and unique feature of the AP1000. Advantages include allowing fine changes of reactivity without changing boron concentration, producing less radioactive effluent, potentially avoiding boron recycling, and reduced operator dose from maintenance of boron equipment. Disadvantages include additional penetrations of reactor vessel head, a potential for reactivity fault from inadvertent withdrawal, and increased dose from control rod drive mechanism maintenance
During load following operations, power system control enables the following load change transients.

- Step load changes of ± 10%
- Ramp load changes of 5% per minute

During daily load follow operations, it allows the following.

- Power ramp from 100% to 50% in 2 hours
- Power remains at 50% for 2-10 hours
- Power ramps up and returns to 100% in 2 hours
- Power remains at 100% for the remainder of the cycle

To preform grid frequency response, the reactor can preform a maximum of 10% power change at 2% per minute.

3 Task 3 - Safety features of the power plant

3.1 Task description

In this task it should be explained what are the general principles of reactor safety. Descriptions of the reactor protection system and engineered safety features should be included. Major results of reactor safety analysis key safety parameters such as, e.g., core damage frequency, should be mentioned.

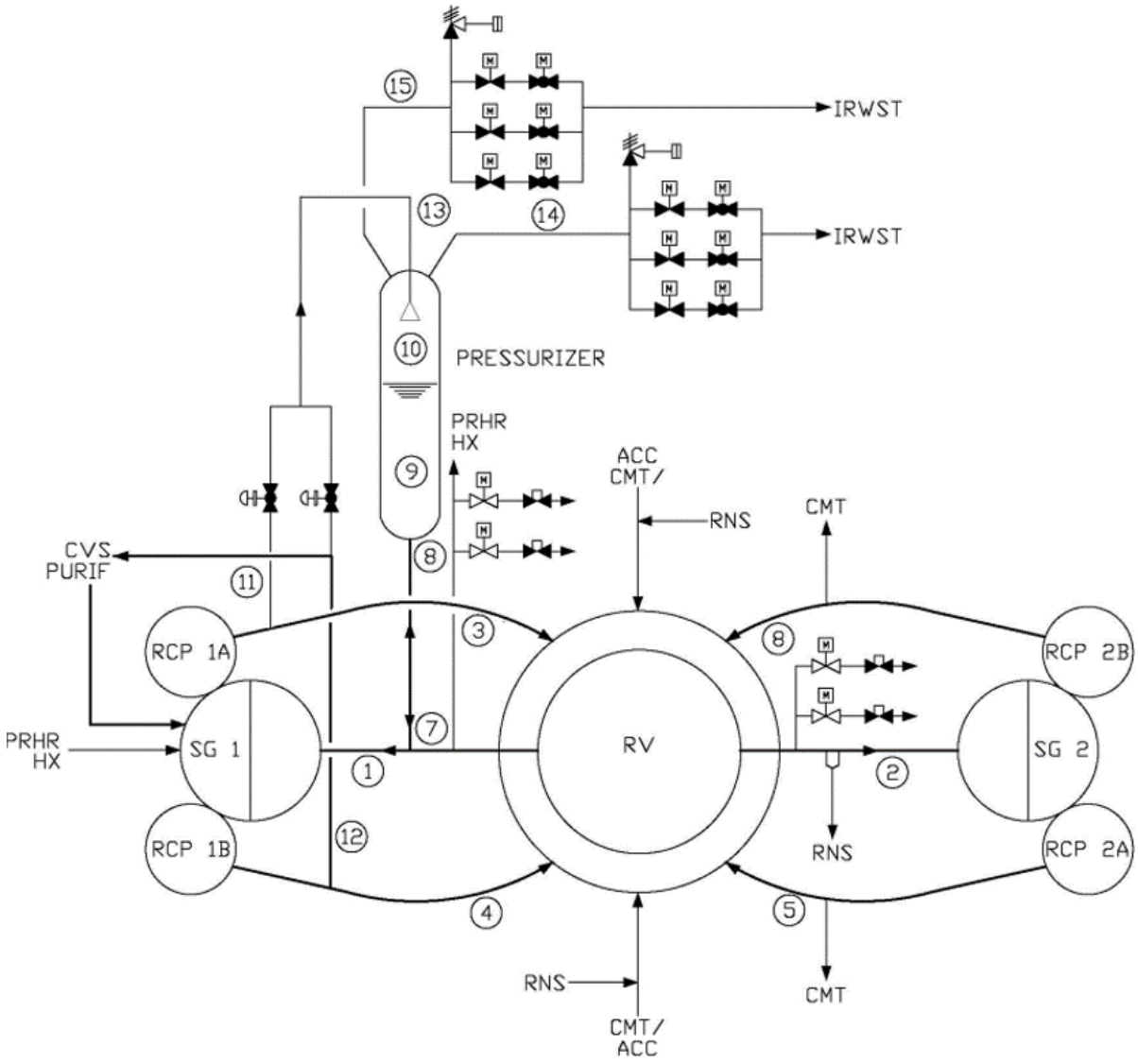

Figure 4: AP1000 primary systems diagram.

3.2 Safety features

Regarding safety principles, the following design aspects contribute to defense-in-depth:

- stable operation,
- physical plant boundaries,
- **passive safety-related systems**,
- diversity within safety-related systems,
- non-safety systems,
- containing core damage.

Some of the safety-related systems in the AP1000 are:

- **passive core cooling system**,
- **passive containment cooling system**,
- containment isolation function,
- passive 1E DC power system,
- main control room emergency habitability system,
- passive containment sump water pH control,
- passive cooling of 1E instrumentation and control areas by the plant structure.

The emergency core cooling system of a typical PWR comes into play during accidents and transients which cannot be handled by the non-safety graded systems. It usually consists of redundant trains of high- and low-pressure safety injections systems driven by pumps, which force water into the primary system to replace core coolant, as in the case of a LOCA. The net result of this approach is a substantial amount of machinery standing by for a call to action that designers and operators work very hard to maintain but never need [2].

The AP1000 passive core cooling system uses staged reservoirs of borated water designed to discharge into the reactor vessel at various threshold state points of the primary system. Figure 5 depicts the main features of the passive core cooling system. There are three sources of borated replacement coolant and three different means of motivating the injection in the core.

- Two core makeup tanks (CMT). Each directly connected to a reactor coolant system (RCS) cold leg by an open pressure balance line. The balance line enters the CMT at the top of the tank, and the system remains static until a pressure difference drives it forward. When actuated, valves are opened, and water is forced out of these tanks into the reactor.
- Two accumulators compressed with nitrogen at 700 PSIG filled with borated water. These are the first to act in case of a Large break LOCAs which cause rapid depressurization.

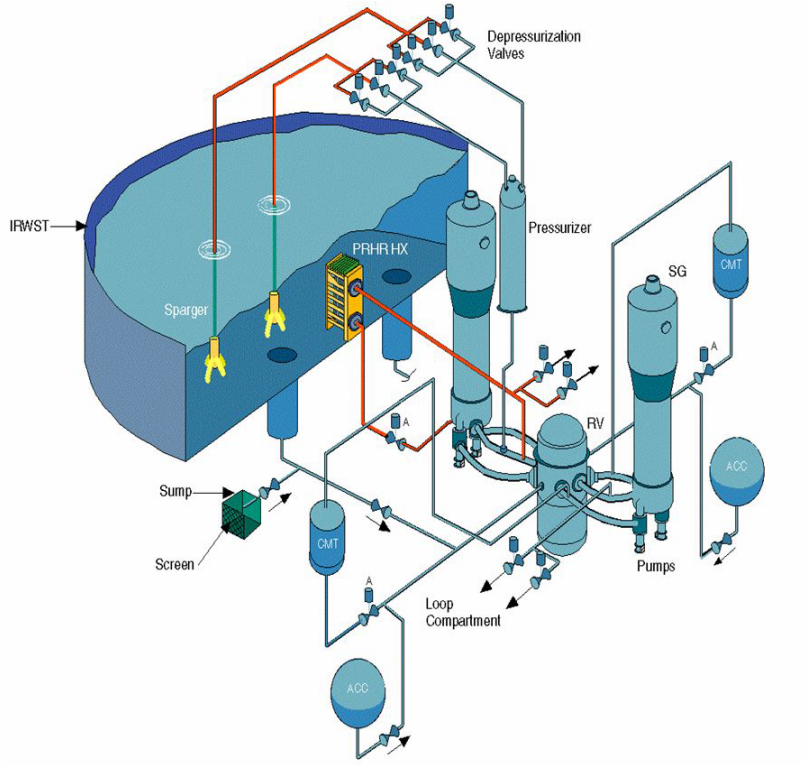

Figure 5: Passive core cooling system AP1000.

- The in-containment refuelling water storage tank (IRWST) located above the RCS piping, will discharge by gravity to the reactor vessel.

All of the passive emergency core cooling systems are located within the containment vessel and there is no need for pumps nor electrical power to maintain operation during an accident. When the signal reaches the actuators, a 1E DC power battery supplies the energy to align the valves in their desired position.

The passive residual heat removal heat exchanger (PRHR HX) is located inside the IRWST and has an inlet from the reactor's coolant system hot leg and an outlet into the RCS cold leg. In case of an accident, or if required by operators, it will absorb heat from the primary system onto the pool until the water begins boiling. The vapor will reach the steel containment inner wall and condense. Through a system of gutters and sumps the condensate will be redirected once again into the IRWST.

In case of an over-pressurization, the depressurization valves directly connected to the pressurizer will discharge steam into the IRWST. Moreover, if needed, the depressurization system will vent to the outside of the reactor containment vessel. Lastly, since the AP1000 has no penetrations along the bottom head, it will retain melted core debris within the reactor vessel. Cooling water from the IRWST can be used to flood the reactor cavity and cool the outside of the reactor vessel.

The steel containment vessel located inside the concrete shield building provides the heat transfer surface necessary to remove heat from inside the containment and

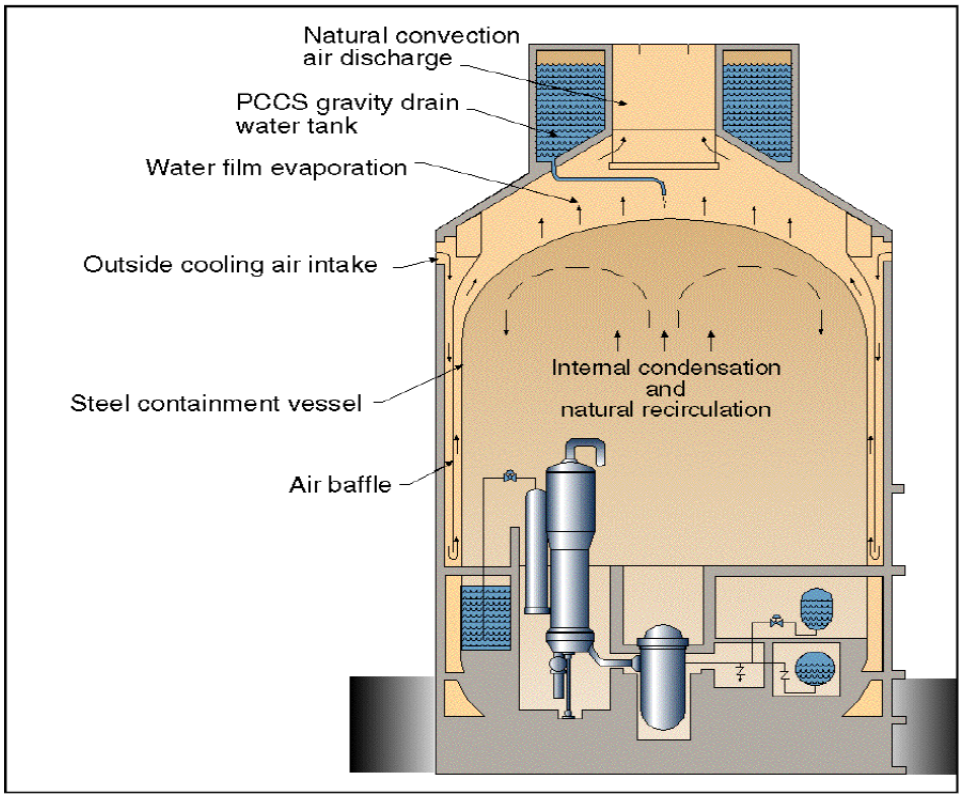

Figure 6: Passive containment cooling system AP1000.

reject it to the atmosphere. This is done by natural circulation of air. During a design basis accident (DBA) the air cooling is supplemented by the evaporation of water. This cooling water drains by gravity from a tank located at the top of the containment shield building and can operate for up to 3 days. The water runs down over the steel containment vessel removing heat from the inside of the vessel [2].

Figure 6 shows the main features of the containment building. Natural air circulation is enhanced by the air intake design of the building, coupled with the air baffles to improve heat transfer. As an extra measure, there is a passive containment cooling ancillary water storage tank located in an ancillary building nearby, which allows the gravity drain water tank to operate for an additional 4 days. From the design it is clear that the ultimate heat sink of the reactor is the atmosphere.

Table 2 illustrates the core melt frequency (CMF) and large release frequency (LRF) per reactor-year, including shutdown events and external events of the AP1000 [7].

Table 2: Key safety parameters

	NRC Requirement, rector/year	**AP1000, rector/year**
CMF	1×10^{-4}	4.2×10^{-7}
LRF	1×10^{-6}	3.7×10^{-8}

4 Task 4 - Calculation of selected core parameters

4.1 Task description

In this task it is required to collect key core parameters. If any of the listed below parameters is not available from the open literature, it should be assumed based on the best knowledge and/or engineering judgement. The minimum list of the required parameters is as follow:

- total core heat output,
- total heat output in fuel pellets (if not known, assume 94.5% of the total core heat output),
- nominal system pressure,
- total core mass flow rate,
- effective fuel cooling mass flow rate (= total mass flow rate minus bypass flow; if not known, assume that core bypass flow is 5% of the total flow),
- number of fuel assemblies,
- active fuel height,
- lattice pitch,
- number of fuel rods per assembly,
- outside fuel rod diameter,
- clad thickness,
- fuel pellet diameter,
- number of spacers, their locations and their local pressure loss coefficients (if not available, assume 6-10 equally-distanced spacers with local loss coefficient of 0.6-0.8 each),
- clad wall roughness.

Using the above input data, the following core-averaged thermal-hydraulic characteristics should be calculated and presented as plots (parameter versus axial distance from the core inlet):

- axial pressure drop distribution,
- axial coolant enthalpy distribution,
- axial coolant temperature distribution,
- flow characteristic of the core, that is the relationship $\Delta p_{core} = f(G_{core})$ - core pressure drop versus mass flux, for core power equal to 0%, 50%, 100%, and 150% of the nominal power, with flow varying from 1% to 150% of the core nominal flow.

In these calculations inlet orifices should be applied (via proper local loss coefficient at fuel assembly inlets) to get about 25% of the total pressure drop in the core just at the inlet orifice. Such inlet orifices are introduced to stabilize flow through the core and avoid hydrodynamic instabilities.

4.2 Description of input data

Table 3: Key core parameters

Parameter	**AP1000**
Total core heat output, MWt	3415
Total heat output in fuel pellets, MWt	3326
Nominal system pressure, MPa	15.513
Total core mass flow rate, m^3/h	80,650
Effective fuel cooling mass flow rate, m^3/h	76,718
Number of fuel assemblies	156
Active fuel length, m	4.3
Lattice pitch, m	1.26×10^{-2}
Number of fuel rods per assembly	264 (17×17 lattice)
Outside fuel rod diameter, m	9.5×10^{-3}
Clad thickness, m	5.72×10^{-4}
Fuel pellet diameter, m	8.1915×10^{-3}
Number of spacers	10 (8 inside active core)
Clad wall roughness, m	3×10^{-7}
Axial peaking factor	1.53
Radial peaking factor	1.75

Table 3 summarizes the main parameters required for the calculation of the required thermal-hydraulic characteristics. The majority of our parameters come from the 2017 Westinghouse AP1000 Pre-construction Safety Report (Cite). This document was part of the licensing process for the design to be accepted by the UK office for nuclear regulation. All others are found in the 2011 NRC Design control document (Cite). All other models and parameters where taken from the course compendium (cite).

4.3 Description of used models and tools

Water properties (density, viscosity, heat capacity, etc.) were taken from the XSteam library in Python (cite). The first step taken during our methodology was dividing the core active height in 1000 nodes of equal height. Water properties are assumed constant within each cell. For the spatial core power distribution, the typical cylindrical core cosine distribution was assumed as

$$q''(r,z) = q''_0 J_0\left(\frac{2.405r}{\tilde{R}}\right) cos\left(\frac{\pi z}{\tilde{H}}\right), \tag{1}$$

where q'' is the heat flux, q''_0 the heat flux at the core center $(r = 0, z = 0)$ J_0 the Bessel function of first kind and zero order, and $\tilde{R}$ and $\tilde{H}$ the extrapolated radius and height respectively. For the reflected core, it can be assumed that $R/\tilde{R} = H/\tilde{H} = 5/6$.

The total reactor power was divided over the number of assemblies and then by the number of rods per assembly, in order to find the power in each fuel rod. This heat output would then be distributed in each cell according to Equation 1. For the average channel, only the axial peaking factor was considered, while for the hot channel both the axial and radial peaking factors were used. The sum of all cells power

output should equal that of the average rod, which was the case for our calculations.

The isolated sub-channel model was considered to find the hydraulic diameter. In this model heat transfer calculations are performed in an averaged, representative "sub-channel" (cite compendium). For a square lattice the hydraulic diameter is given by

$$D_h = d_r \left[\frac{4}{\pi} \left(\frac{p}{d_r} \right)^2 - 1 \right], \tag{2}$$

where p is the lattice pitch and d_r the rod diameter. Additionally, a second relationship can be used to find the cross-sectional area

$$D_h = \frac{4A}{P_w}, \tag{3}$$

where A is the sub-channel cross-sectional area, and P_w is the channel's wetted perimeter. Equations 2 and 3 were used to find the hydraulic diameter and channel cross-sectional area respectively.

The next parameters we will define are the dimensionless quantities needed. First, the Reynolds number helps predict fluid flow patterns by measuring the ratio between inertial and viscous forces (cite). The equation used during our calculations was

$$Re = \frac{\rho u L}{\mu}, \tag{4}$$

where ρ is the density of the fluid, u is the flow speed, μ is the dynamic viscosity of the fluid, and L is the characteristic linear dimension (i.e., hydraulic diameter in our case). Next, the Prandtl number defines the ratio of momentum diffusivity to thermal diffusivity (cite), and it is given by

$$Pr = \frac{c_p \mu}{\lambda_l}, \tag{5}$$

where c_p is the specific heat and λ_l is the thermal conductivity of the liquid. Finally, the Nusselt number is the ratio of convective to conductive heat transfer at fluid boundaries. For clad-coolant heat transfer in channels with single phase flow, the following Dittus & Boelter correlation was applied

$$Nu = 0.023 \times Re^{0.8} Pr^{0.4}, \tag{6}$$

which is valid for $L/D_h > 60$, $Re > 10^4$ and $0.7 < Pr < 100$. For turbulent flow in commercial rough pipes, the Colebrook formula is defined as

$$\frac{1}{\sqrt{C_f}} = -4.0 \log_{10} \left(\frac{k/D_h}{3.7} + \frac{1.255}{Re\sqrt{C_f}} \right), \tag{7}$$

where C_f is the Darcy friction factor and k is the wall roughness. Equation 7 was solved through the Lambert W function (also called omega function) (cite). Lastly, the Fanning friction factor is simply obtained by dividing the Darcy friction factor by 4.

The enthalpy at the inlet of the reactor core was found through the water properties at inlet, which are known. From then on, the change in enthalpy is calculated in each cell by

$$\frac{di(z)}{dz} = \frac{q'' P_H(z)}{W}, \tag{8}$$

where W is the mass flow rate and P_H the heated perimeter. A similar procedure is done for the calculation of the temperature in each cell. The inlet temperature is known and the change is found through the pyXSteam library with the enthalpy of the cell and the pressure.

The equilibrium quality is calculated in each cell to check whether we have single- or two-phase conditions. Knowing the equilibrium quality at inlet we calculate the change in each cell as

$$x_{ex} \equiv \frac{i(z) - i_f}{i_{fg}} \tag{9}$$

where i_{fg} is the difference between the vapor phase saturation enthalpy and the liquid phase saturation enthalpy.

Finally, the homogeneous equilibrium model (HEM) was used to calculate the void fraction. This model assumes both phases are in the same thermodynamic equilibrium and flow with the same speed (Cite).

$$\alpha(z) = \begin{cases} 0 & x_e \leq 0 \\ \frac{1}{1+\frac{\rho_g}{\rho_f}\left(\frac{1-x_e(z)}{x_e(z)}\right)} & 0 < x_e < 10 \\ 1 & x_e \geq 1 \end{cases}$$

The first terms we found for the pressure drop calculation were the local losses, also known as minor head losses. This pressure drops are a function of flow regime, flow velocity and the geometry of the given components, components such as bends, fittings, valves, inlet orifices, etc. The exit loss coefficient was found to be

$$-\Delta p_E = \xi_{ex} \frac{G^2}{2\rho}; \xi = 1.0,$$

while the loss coefficient for each spacers was taken as

$$\xi_{spacer} = 1.95 Re^{-0.08}.$$

It must be pointed out that the AP1000 has 4 intermediate flow mixers (IFM) to improve the heat transfer. However, these were ignored because no loss coefficient from them could be found in the literature, and instead we assumed 8 evenly distributed spacers inside the active core. Knowing the value of the loss coefficients we still need the local multiplier for the two-phase pressure drop calculations. This multiplier is given by

$$\phi^2_{lo,d} = \left[1 + \left(\frac{\rho_f}{\rho_g} - 1\right) x\right].$$

Finally, the inlet orifice pressure loss is defined as

$$-\Delta p_{orifice} = \xi_{orifice} \frac{\rho U^2}{2} = \xi_{orifice} \frac{G^2}{2\rho}. \tag{10}$$

The value of the loss coefficient from Equation 10 for a PWR operating at nominal conditions contributes to around 25% of the total pressure drop. Therefore, an initial calculation of the pressure drop was made before finding the value of the coefficient and integrating it into the total pressure drop.

The two-phase pressure drop can be easily compared with the single-phase pressure drop with the use of the friction, gravity, and acceleration multiplier. The friction multiplier can be found as a function of the local equilibrium quality from

$$\phi_{lo}^2 = \left[1 + \left(\frac{\mu_f}{\mu_g} - 1\right) x\right]^{-0.25} \left[1 + \left(\frac{\rho_f}{\rho_g} - 1\right) x\right], \tag{11}$$

by integrating over the channel length we obtain

$$r_3 = \frac{1}{L} \int_0^L \phi_{lo}^2 dz. \tag{12}$$

The gravity pressure drop multiplier is given as

$$r_4 = \frac{1}{L\rho_f} \int_0^L \left[\alpha\rho_g + (1-\alpha)\rho_f\right] dz, \tag{13}$$

whereas the acceleration multiplier is

$$r_2 \equiv \rho_f \int_0^L \frac{d}{dz} \left[\frac{x^2}{\alpha\rho_g} + \frac{(1-x^2)}{(1-\alpha)\rho_f}\right] dz. \tag{14}$$

Lastly the single-phase pressure drop is

$$-\Delta p = \frac{4C_f L}{D} \frac{G^2}{2\rho_f} + L\rho_f g \sin\varphi, \tag{15}$$

while the two-phase pressure drop is found from

$$-\Delta p = r_3 C_{f,lo} \frac{4L}{D} \frac{G^2}{2\rho_f} + r_4 L\rho_f g \sin\varphi + r_2 \frac{G^2}{\rho_f} + \left(\sum_{i=1}^{N} \phi_{lo,d,i}^2 \xi_i\right) \frac{G^2}{2\rho_f}. \tag{16}$$

The pressure drop was calculated from Equations 15 and 16 depending on the quality of the cell. As previously stated the first iteration was made to find the inlet orifices pressure loss from Equation 10, then with this local loss added, the pressure was iterated until its final value.

4.4 Presentation of results

As it was mentioned before, the power distribution in the core was found through Equation 1 and is shown in Figure 7, where it has the expected cosine shape.

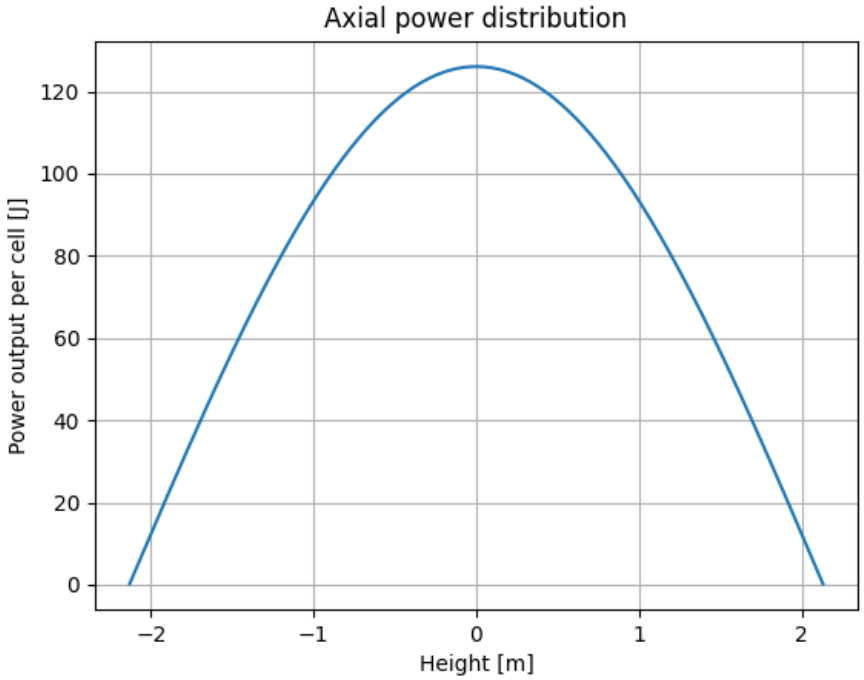

Figure 7: Axial power distribution in the average channel.

The axial coolant enthalpy is calculated in each cell with Equation 8 and is depicted in Figure 8.

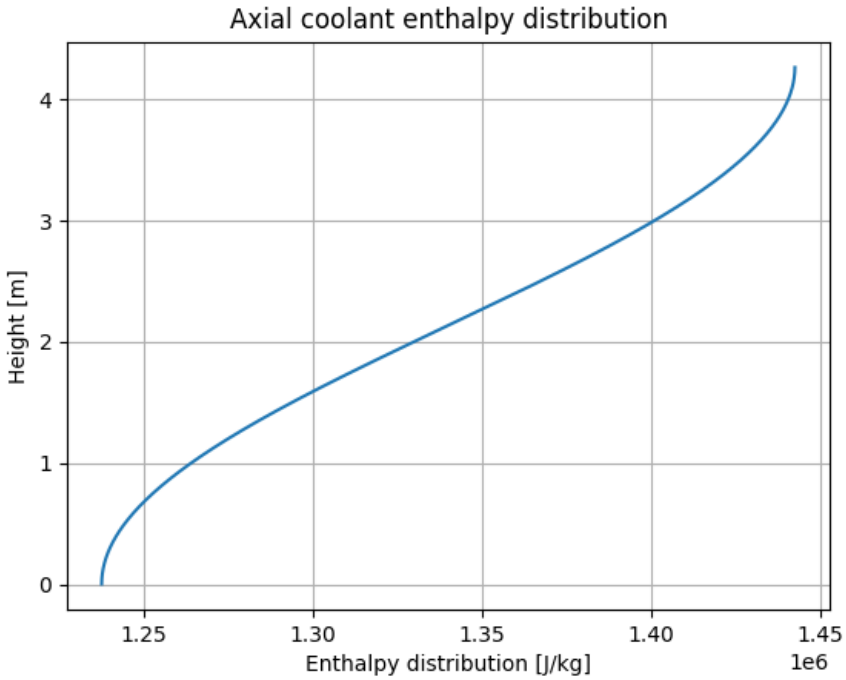

Figure 8: Axial coolant enthalpy distribution in the average channel.

The temperature of each node is calculated through XSteam with the pressure and enthalpy of each node. Figure 9 shows the temperature distribution.

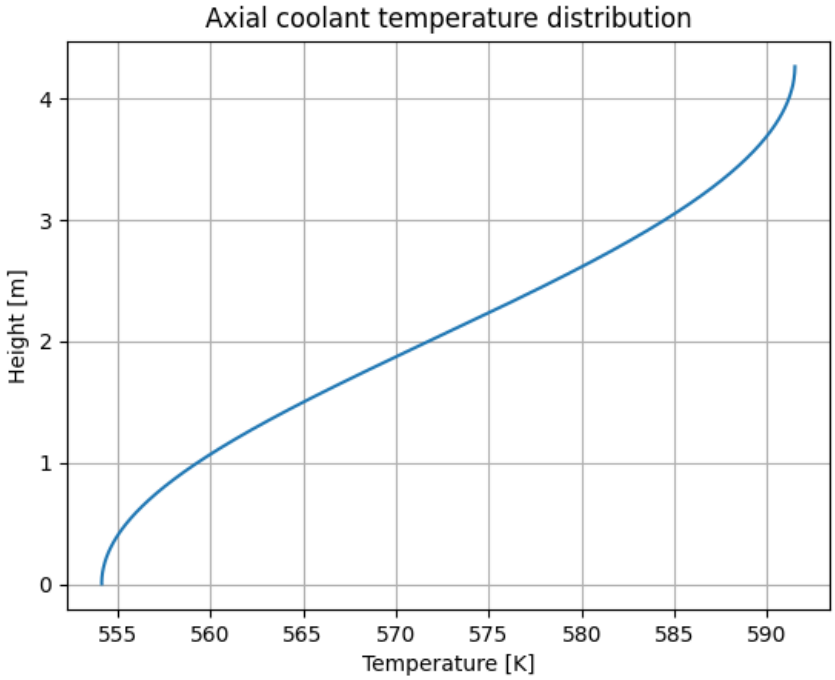

Figure 9: Axial coolant temperature distribution in the average channel.

Adding up all the local, friction, acceleration, and gravity contributions and applying either the single- or two-phase pressure drop equation, was the procedure followed for calculating the pressure drop, which is shown in Figure 10.

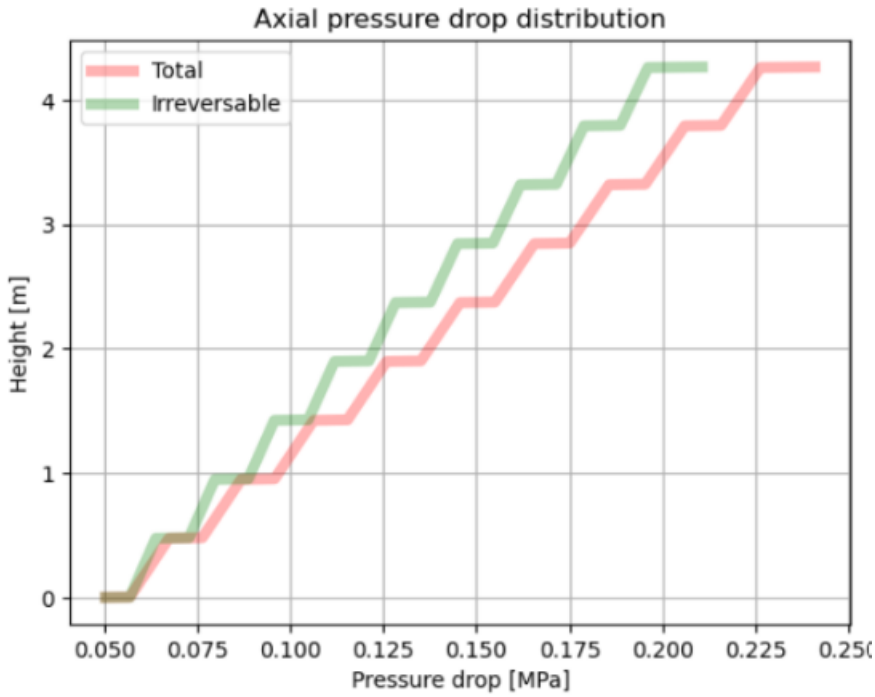

Figure 10: Total pressure drop in the core.

Finally, the pressure drop of different power percentages, with varying nominal flow rates were calculated to present the flow characteristic curves in Figure 11.

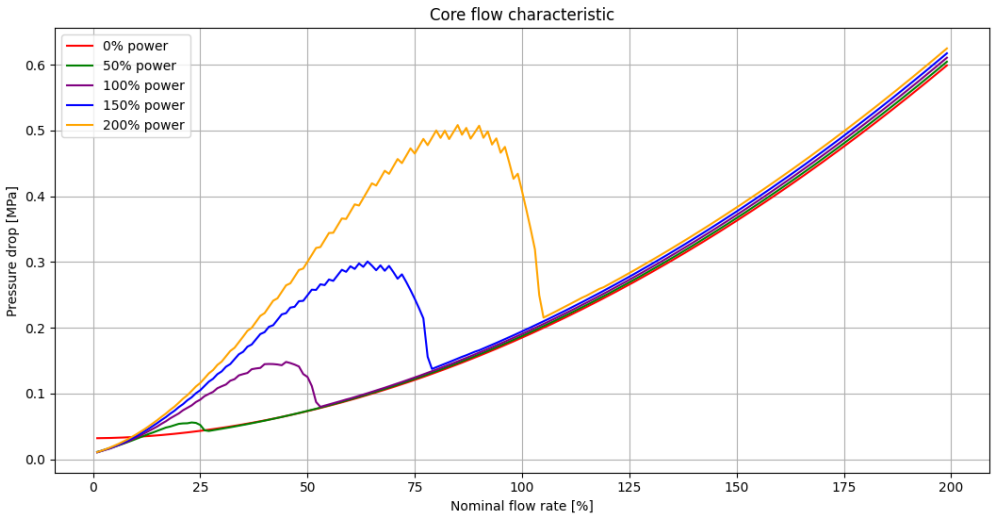

Figure 11: Flow characteristic of the core.

4.5 Discussion of the results and conclusions

Once again, the axial power distribution from Figure 12 is what we expect because of the cosine distribution used. The first and last cells have almost 0 Joules of power output because of the number of nodes used. Looking at the axial coolant enthalpy

and temperature distribution shown in Figures 8 and 9, they have a steeper change in the middle because of the way the power is distributed in the core.
Regarding the pressure drop distribution we can clearly see the contribution of the spacers and the inlet orifice. The calculated value closely resembles that reported by Westinghouse of 0.26±MPA (cite).
Lastly, the core characteristic graph shown in Figure 11 can be clearly divided in two regions. At 0% power the only contribution to the pressure drop is the hydro static pressure which is higher at first, but is overtaken by the friction contribution at around 10% nominal flow. At these low flows, since the fluid is rapidly being turned into steam, we see the pressure drop rise up. This is because both the acceleration and the friction pressure drops increase in two-phase flow due to the lower pressure of the steam. As we increase the nominal flow rate, for any given power the total pressure drop is relatively similar.

5 Task 5 - Calculation of CHF margins in a hot channel

5.1 Task description

We were directed to find the CHF (Critical Heat Flux). This is one of the factors that limit the maximum thermal power in the core. To do this we were instructed to find the margins to the CHF occurrence as estimated for a hot channel. In PWRs the DNB (Departure from Nucleate Boiling) should be assumed and the following parameters should be found:

- Axial pressure drop distribution.
- Axial coolant enthalpy distribution.
- Axial coolant temperature distribution.
- Axial distribution of DNBR (Departure from Nucleate Boiling Ratio) and axial location of MDNBR [6].

5.2 Description of input data

5.3 Description of used models and tools

To find the temperature in the hot channel, the cosine power distribution defined in Eq. 1 was combined with this equation for finding f_R, the radial peaking factor

$$f_R(z_P) = \frac{q'''(0, z_P)}{\frac{1}{\pi R^2}\int_0^R q'''(r, z_P) 2\pi r dr}. \tag{17}$$

By multiplying the axial and radial peaking factors given in Tab. 3, Eq. 1 yields the power distribution in the hot channel of the core, with is in the center. After finding this new, higher power distribution, the calculations of Section 4.3 were repeated to find axial pressure drop, axial enthalpy distribution, and axial temperature distribution. With these new values, we then used the Reddy and Fighetti generalized sub-channel critical heat flux (CHF) correlation to find CHF, $q''_{cr}(r)$. This equation has a base form of

$$q''_{cr}(r) = B\frac{A - x_{in}}{C + \frac{x(r)-x_{in}}{q''_R(r)}} \tag{18}$$

that combines the following factors

$$A = a_1 p_R^{a_2} G_R^{(a_3 + a_4 p_g)},$$
$$B = 3.1544 \times 10^6,$$
$$C = c_1 p_R^{c_2} G_R^{(c_3 + c_4 p_g)},$$
$$G_R = G/1356.23,$$
$$p_R = p/p_{cr}$$

and,

$$q''_r(r) = q''(r)/3.1544 \times 10^6.$$

In Eq. 18, x_{in} is the inlet equilibrium quality,r is axial location, G is the mass flux in kg/m^{2}s, p is pressure in Pa and p_{cr} is critical pressure in Pa. The additional

factors are $a_1 = 0.5328, a_2 = 0.1212, a_3 = -0.3040, a_4 = 0.3285, c_1 = 1.6151, c_2 = 1.4066, c_3 = 0.4843$, and $c_4 = -2.0749$. This correlation is valid for these conditions $147 < G < 3023$ kg/m^{2}s, $13.8 < p < 169.9$ bar, $8.9 < D_h < 13.9$ mm, $6.3 < D_H < 13.9$ mm, $-0.25 < x < 0.75$, $-1.1 < x_{in} \leq 0$, and $0.762 < L < 4.267$m. D_h is the hydraulic diameter of the sub-channel and D_H is the heated diameter. Both of these are equal because we are not accounting for any unheated portions of the fuel assemblies.
To determine if there is departure from nucleate boiling in the hot channel, the ratio of CHF $q"_{cr}(z)$ and actual heat flux : $q"(z)$ was found. This ratio,

$$DNBR = \frac{q"_{cr}(z)}{q"(z)} \tag{19}$$

is called the departure from nucleate boiling ratio (DNBR), and when it is equal to one, departure from nucleate boiling occurs. The minimum point of the DNBR is the minimum DNBR (MDNBR) and is the location where the fuel assembly is closest to departure from nucleate boiling and needs to be found to predict thermal margins.

5.4 Presentation of results

The axial power distribution of the hot channel, shown in Fig. 15, shows how the power has increased compared to the average channel. The change in pressure drop is shown in Fig. 13 and the change in enthalpy is shown in Fig. 14. Fig. 19 shows the change in temperature. In Fig. 16 the CHF and the heat flux in the hot channel are compared, and the DNBR is plotted. MDNBR was found to be 1.33 at 2.68 m, in the second half of the fuel assembly length. In the hot channel, the quality stayed below 0, so two-phase flow was not considered.

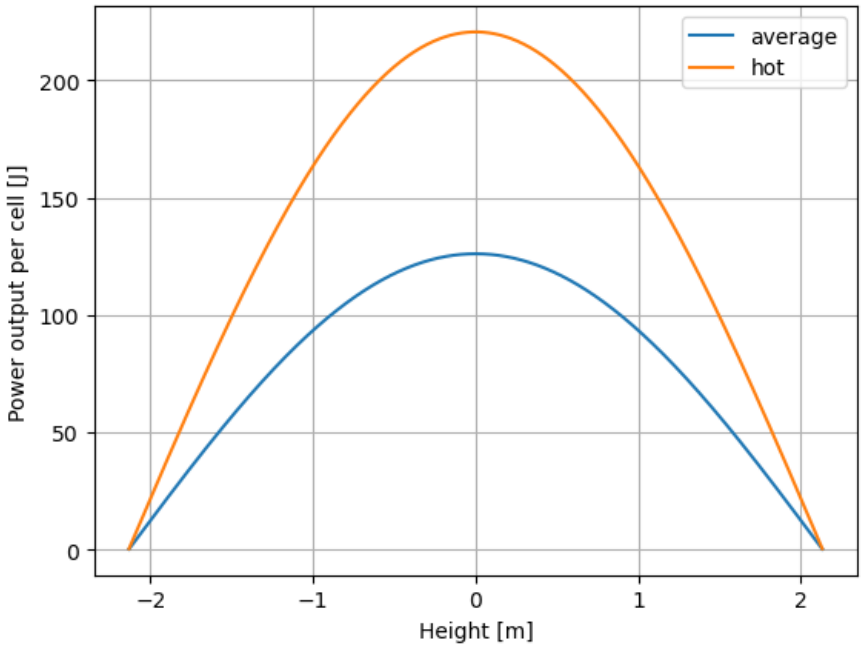

Figure 12: Axial power distribution in average and hot channel.

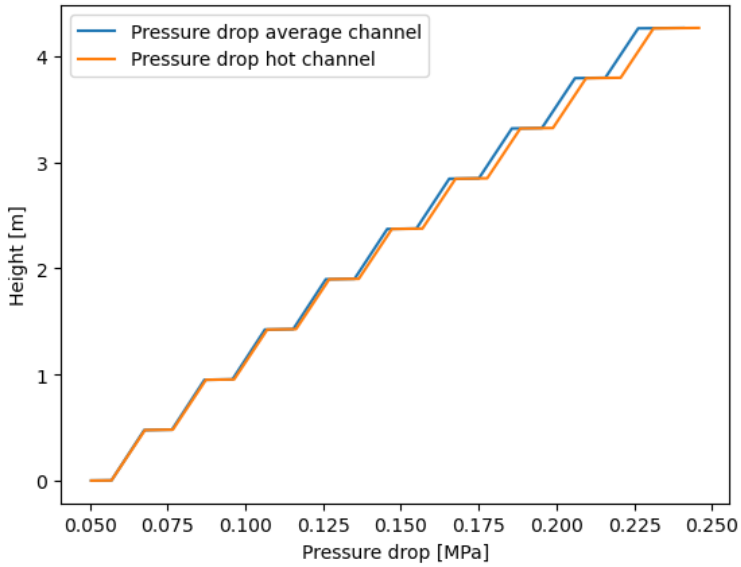

Figure 13: Axial pressure drop in average and hot channel.

5.5 Discussion of the results and conclusions

In each of the plots comparing average chanel to hot channel is can be seen that the increase in power in the hot channel also increases other parameters for that channel. The channel does not reach two phase flow which is typical of PWRs. The calculated MDNBR of 1.33 at 2.68 m is similar to the MDNBR at nominal conditions of 2.80 [8]. This difference is possibly due to the cosine power distribution used potentially having a larger peak than the actual power distribution used in the AP1000. The MDNBR is downstream of the hot spot caused by the heat flux location due to the increase in enthalpy downstream, which is typical.

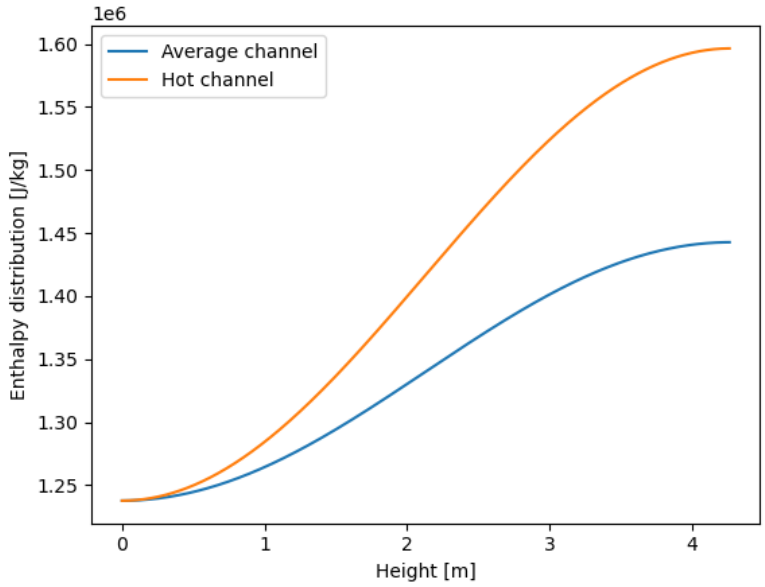

Figure 14: Axial enthalpy distribution in average and hot channel.

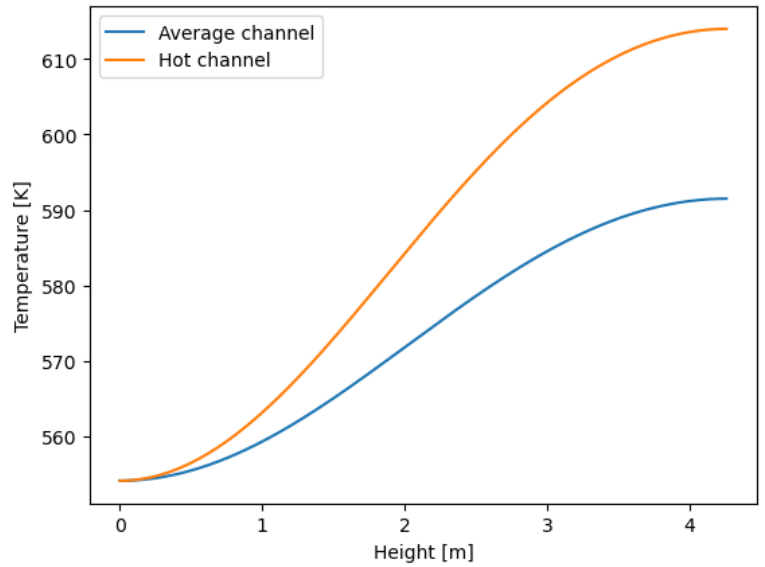

Figure 15: Axial temperature distribution in average and hot channel.

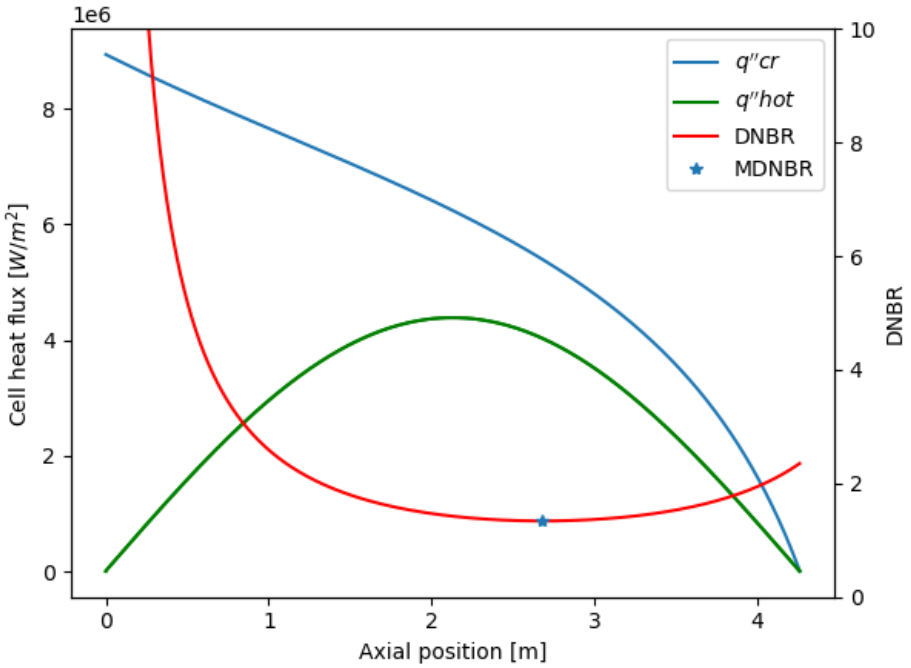

Figure 16: Flux, DNBR, and MDNBR compared to axial position.

6 Task 6 - Calculation of the maximum cladding and fuel pellet temperature

6.1 Task description

In this task we were directed to verify that the fuel temperature would not exceed the melting point of the fuel material at any point in the reactor and that the cladding temperature did not exceed the maximum allowed for the cladding material. Additionally, we needed to identify the locations for the hottest fuel and cladding. To do this, we assumed the fuel was as-fabricated, but the materials used were as realistic as possible.

6.2 Description of input data

The fuel and cladding parameters from Tab. 3 were used, along with the hot channel parameters calculated in Section 5. The fuel cladding material is ZIRLO, which we assumed has similar properties to Zircaloy-4. The fuel is uranium oxide [8].

6.3 Description of used models and tools

To find the clad maximum temperature, the heat transfer coefficent was calculated using the Dittus and Boelter correlation from Eq. 6 was used with the bulk fluid temperature T_{lb} calculated in Section 5 and plotted in Fig. 15 in Newton's equation for convective heat transfer to find T_{Co}, the cladding surface temperature. Newton's equation for convective heat transfer is

$$T_{Co} = \frac{q''}{h} + T_{lb}. \tag{20}$$

To find the maximum temperature of the fuel, coefficients for the thermal conductivity of the cladding λ_C, the gas gap λ_G, and the fuel λ_F were required. For the Zircoloy-4 cladding

$$\lambda_C = 12.6 + 0.0118 \times T$$

where T is the temperature of the cladding in °C, valid between 20-800°C. For the gas gap, we assumed that it was filled with helium, and used

$$\lambda_G = 3.366 \times 10^{-3} \times T^{0.668}$$

and for the fuel we assumed that is was solid UO_2 with 95% density and used

$$\lambda_F = \frac{100}{7.5408 + 17.692 \times t + 3.6142 \times t^2} + \frac{6400}{t^{5/2}} \times \exp\frac{-16.35}{t}$$

where $t = T/1000$. These correlations were then used with the equation

$$\Delta T = \frac{q'}{4\pi}\left[\frac{1}{\lambda_F} + \frac{2}{\lambda_G}\ln\left(\frac{r_{Go}}{r_{Fo}}\right) + \frac{2}{\lambda_C}\ln\left(\frac{r_{Co}}{r_{Go}}\right) + \frac{2}{r_C oh}\right]$$

To find the heat transfer coefficients, the temperature was iterated 5 times for each, starting with the temperature of the previous material.

6.4 Presentation of results

The maximum cladding temperature in the hot channel was 393 °C at axial position 2.63 m. The temperature distribution of the cladding can be seen in Fig. 17. The maximum fuel temperature was calculated to be 2343 °C at position 2.148 m, and can be seen in Fig. 18. The radial distribution of temperature within the hot channel at position 2.148 m is seen in Fig. 19.

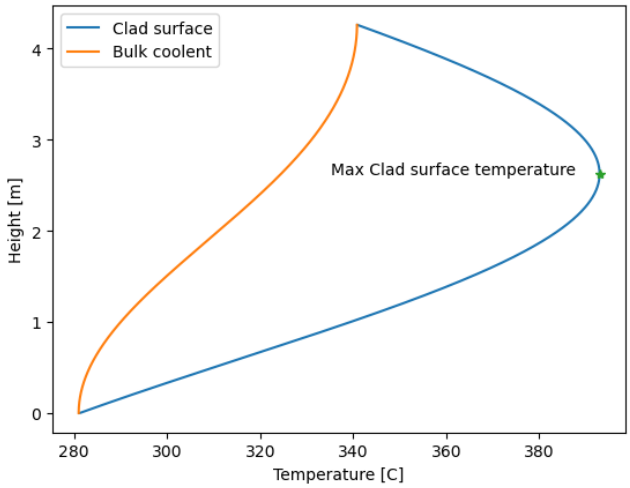

Figure 17: Cladding temperature distribution.

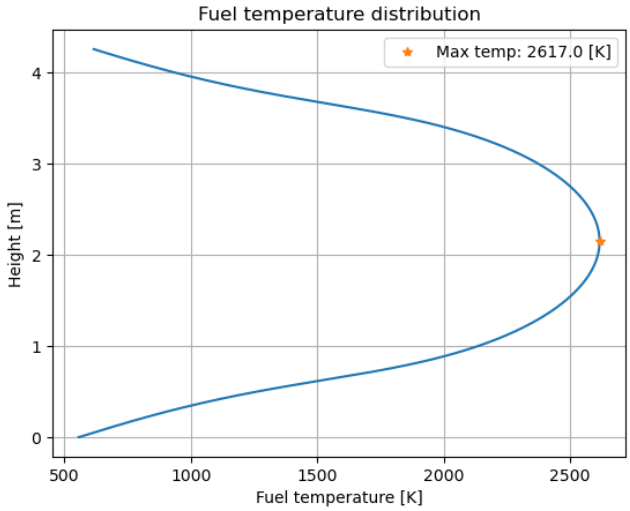

Figure 18: Fuel center-line temperature distribution in hot channel.

6.5 Discussion of the results and conclusions

These results show that at the hottest points in both the fuel and cladding, the design limits were not exceeded. The design maximum temperature for the cladding is 1200°C, so the calculated maximum of 393 °C is significantly lower. The maximum design temperature of the fuel is 2593.33°C, so the calculated maximum of 2343°C

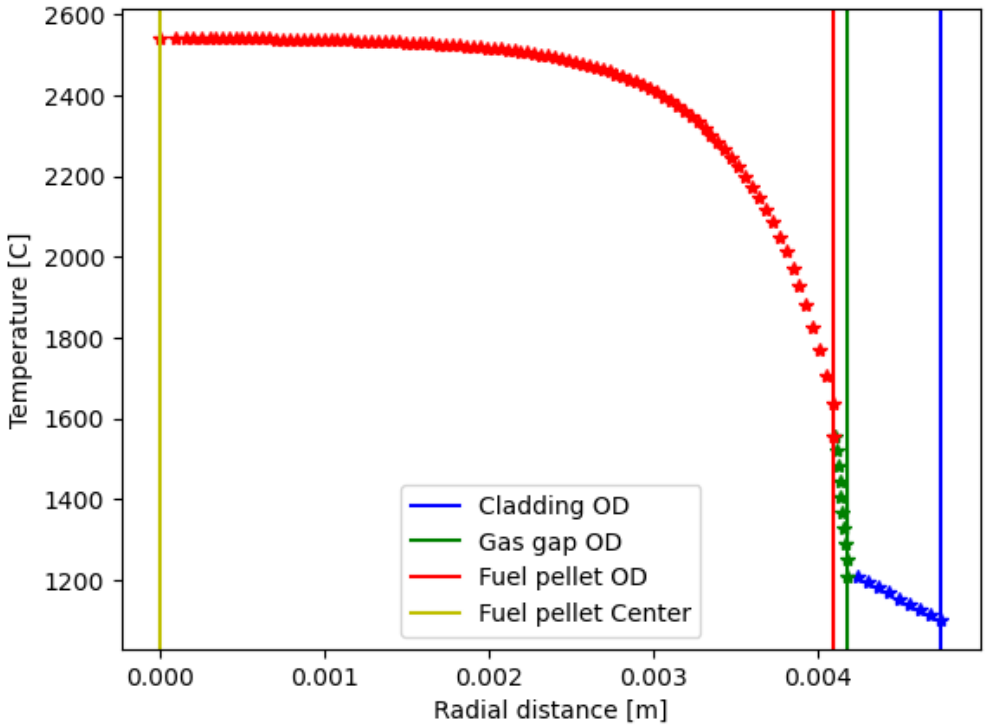

Figure 19: Radial temperature distribution.

is also significantly lower. The large number of correlations required to calculate the fuel center line temperature could be a source of error.

7 Bibliography

References

[1] WestinghouseAP1000. *AP1000 Station Blackout - Passive Core Cooling*. 2014. URL: https://www.youtube.com/watch?v=FCorzfw5liQ (visited on 02/11/2023).

[2] Paolo Gaio. *AP1000 The PWR Revisited*.

[3] *AP1000 — NRC.gov*. URL: https://www.nrc.gov/reactors/new-reactors/large-lwr/design-cert/ap1000.html (visited on 01/26/2023).

[4] *Coping with Station Blackout.pdf*. Apr. 2011.

[5] *AP1000 Plant. Passive Safety Systems and Timeline for Station Blackout*. 2021.

[6] *SH2702-VT23 Project work description*.

[7] *AP1000 Pressurized Water Reactor — Westinghouse Nuclear*. URL: https://www.westinghousenuclear.com/energy-systems/ap1000-pwr (visited on 01/26/2023).

[8] Westinghouse. *Westinghouse AP1000 Design Control Document Rev. 19*. ML11171A500. NRC, June 21, 2011. URL: https://www.nrc.gov/docs/ML1117/ML11171A500.html (visited on 02/02/2023).